

Article

A Study on Weight Reduction and High Performance in Separated Magnetic Bearings

Si-Woo Song ¹, Won-Ho Kim ², Ju Lee ¹ and Dong-Hoon Jung ^{3,*}¹ Department of Electrical Engineering, Hanyang University, Seoul 04763, Republic of Korea² Department of Electrical Engineering, Gachon University, Seongnam 13120, Republic of Korea³ Department of Mechanical, Automotive and Robot Engineering, Halla University, Wonju 26404, Republic of Korea

* Correspondence: dh.jung@halla.ac.kr

Abstract: Recently, high-speed motors are receiving a lot of attention in the industrial field. When driving a motor at high speed, the advantages include high power density, high efficiency, and miniaturization. However, the disadvantages of the high-speed operation of motors are mechanical and structural safety. This is because the bearings used in high-speed motors require characteristics such as precision and low friction. There are two prominent types of bearings mainly used in high-speed motors: rolling bearings and magnetic bearings. A feature of rolling bearings is that they reduce frictional resistance by contacting points or lines between the shaft and the bearing. However, the disadvantages of rolling bearings are high mechanical friction losses due to the need for contact with the lubrication system. Maintenance costs are high. For this reason, a lot of research on bearings is being conducted to reduce the frictional loss of bearings and increase their efficiency and reliability. Bearings that are advantageous for high-speed operation are magnetic bearings that do not require lubricants, have no friction loss, and have low maintenance. However, magnetic bearings have disadvantages such as high cost and difficulty in miniaturization. In this paper, a stator with a separated teeth structure was used to compensate for these disadvantages. Using this, a model with miniaturization, light weight, and high manufacturability was proposed. The model name proposed in this study is called the STMB (separated teeth magnetic bearing). There are also disadvantages of the STMB model proposed in this paper. A model that compensates for this drawback is called the HSTMB (hybrid separated teeth magnetic bearing). The HSTMB reduces the weight by removing the back yoke of the stator and has advantages of a high filling rate and high productivity in the form of a module. As a result, high productivity, light weight, and high performance are possible when the HSTMB is applied, which was proven through FEA (finite element analysis).

Keywords: PM; magnetic bearing; bearing; weight reduction; force; magnet; separated stator; stiffness; hybrid



Citation: Song, S.-W.; Kim, W.-H.; Lee, J.; Jung, D.-H. A Study on Weight Reduction and High Performance in Separated Magnetic Bearings. *Energies* **2023**, *16*, 3136. <https://doi.org/10.3390/en16073136>

Academic Editor: Marcin Kaminski

Received: 23 February 2023

Revised: 21 March 2023

Accepted: 28 March 2023

Published: 30 March 2023



Copyright: © 2023 by the authors. Licensee MDPI, Basel, Switzerland. This article is an open access article distributed under the terms and conditions of the Creative Commons Attribution (CC BY) license (<https://creativecommons.org/licenses/by/4.0/>).

1. Introduction

Technical demands for high speed, light weight, high power, and high efficiency are emerging in various motor fields. In the field of motors, permanent magnet motors are of great interest for the technical requirements for high-speed operation. In research for the high-speed operation of motors, electromagnetic design is important, but mechanical and structural reliability are also important factors [1–4]. Therefore, in order to reduce frictional loss of mechanical parts and increase efficiency and reliability, a lot of research on bearings is being conducted [5–9]. Bearings commonly used in high-speed motors require precision, high speed, minimum displacement, and small friction loss. Bearings commonly used in high-speed motors include rolling bearings (RB) and magnetic bearings (MB). Among the two bearings, the rolling bearing can reduce frictional resistance because it is in contact with the point or line between the shaft and the bearing. However, since

contact is essential in rolling bearings, mechanical friction loss occurs and maintenance costs are high. In addition, the rotational speed is limited due to contact between the bearing and the shaft. On the other hand, magnetic bearings do not require lubrication, have no frictional losses, and have low maintenance costs. In addition, since there is no mechanical friction, there is no limit to the rotational speed, so it has many advantages over mechanical bearings [10–14]. Magnetic bearings are widely used in industrial applications such as turbo compressors, vacuum technology, and flywheel [15–17] technology due to these advantages. Magnetic bearings have many advantages, but they are difficult to use. This is because they are expensive and difficult to control and miniaturize. High-speed motors are easy to design for miniaturization, but magnetic bearings are difficult to miniaturize, so the set becomes large [18–23]. Therefore, this paper proposes a new magnetic bearing capable of miniaturization and light weight by using a stator with a separated teeth structure. The separated teeth structure [24] model proposed in this study is the STMB (separated teeth magnetic bearing). When the back yoke is removed and the teeth are separated, new parts appear, which are called lips. The weight of the existing stator is mostly controlled by the back yoke. The STMB can reduce the weight by removing the back yoke. The STMB has a modular structure. Therefore, it has the advantage of having a high fill factor. However, the STMB has a large magnetic leakage flux between stator modules and a small effective air gap, so performance is not high. Therefore, in this paper, the HSTMB (hybrid separated teeth magnetic bearing) is finally proposed. The HSTMB has the effect of reducing magnetic leakage flux and increasing the effective air gap area by inserting a magnet into the shoe part of the stator [25].

2. Analysis of Existing Model Specifications

Figure 1 shows the existing model and the magnetic flux line of the existing model. The existing model is a magnetic bearing with four teeth. Table 1 shows the existing model specifications. The outer diameter of the stator of the existing model is 40 mm, and the outer diameter of the rotor is 12 mm. In addition, the air gap was selected as 0.5 mm, and the winding per tooth was selected as 35. At this time, the current density was selected based on 3A, and 10.6 A/mm² was selected based on 3A. At this time, Figure 1b aligns with the magnetic flux and makes a magnetic equivalent circuit.

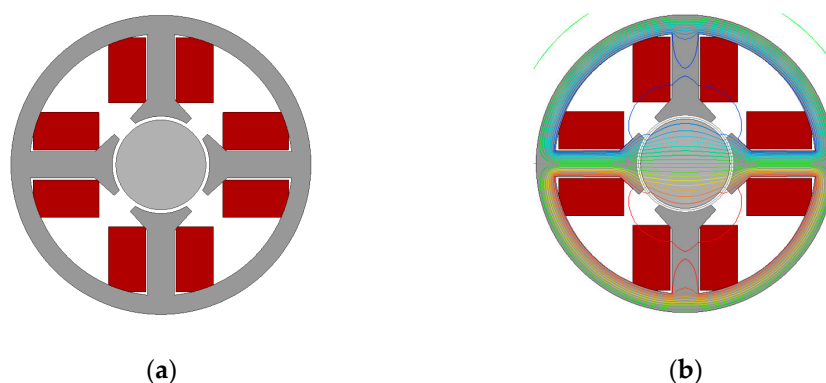


Figure 1. Magnetic flux line of the conventional model and the conventional model: (a) conventional model and (b) magnetic flux line of the conventional model.

Table 1. Conventional model specification.

Parameter	Value	Unit
Stator diameter	40	mm
Rotor diameter	12	mm
Air gap	0.5	mm
Turn	35	-
3A of current density	10.6	A/mm ²

The static magnetic circuit model of the conventional model is shown in Figure 2, where N_r is the number of radial coil turns, and I_x and I_y are the radial control currents. R_{gx+} , R_{gx-} , R_{gy+} , and R_{gy-} , are the reluctances of radial air gaps in the $x+$, $x-$, $y+$, and $y-$ directions, respectively. This kind of model does not take the eddy current effects and leakage effects into consideration, so the accuracy of the model is not high. Based on this, current stiffness and displacement stiffness were analyzed. The resistance and flux formulas are shown below.

$$\begin{aligned} R_{x+} &= \frac{g+x}{\mu_0 A_r}, R_{x-} = \frac{g-x}{\mu_0 A_r}, \\ R_{y+} &= \frac{g+y}{\mu_0 A_r}, R_{y-} = \frac{g-y}{\mu_0 A_r}, \end{aligned} \quad (1)$$

$$\phi_{ix} = \phi_{ix-} = \frac{2N_r i_x}{R_{y+} + R_{y-}}, \quad (2)$$

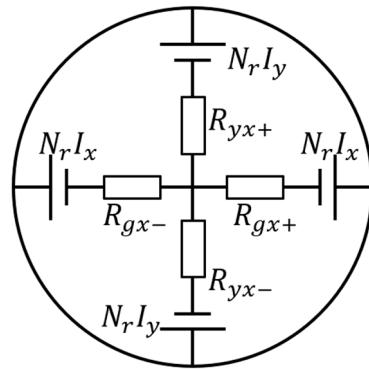


Figure 2. Conventional model magnetic equivalent circuit.

In Equation (1), μ_0 is the permeability of vacuum, A_r is the area where magnetic flux flows, N_r is the number of windings turns, and g is the air gap length. The radial force is expressed in Equation (3):

$$f_x = \frac{1}{2\mu_0 A_r} ((\phi_{ix+} + \phi_{ix-})^2) \quad (3)$$

In Equation (3), ϕ_{ix} represents the magnetic flux in x -axis. The radial force can be expressed as in Equation (4):

$$f_x = k_{ri} i_x + k_r x \quad (4)$$

In Equation (4), k_{ri} means current stiffness and k_r indicates displacement stiffness. At this time, it was compared through FEM and magnetic equivalent circuit analysis. FEM and magnetic equivalent circuit analysis, as shown in Figure 3.

Current stiffness is shown in Figure 3a. At this time, the FEM analysis and the magnetic equivalent circuit analysis showed the magnetic force according to the control current. Looking at the magnetic equivalent circuit analysis, the magnetic force tends to increase uniformly as the control current increases. However, the FEM analysis has a different tendency. When the control current increases, the magnetic force also tends to increase, but it was confirmed that it does not increase uniformly like the magnetic equivalent circuit analysis. The reason is the presence of magnetic leakage flux and saturation in the core. Looking at 7A~8A, it can be seen that the width of the increase in the magnetic force is decreasing. This cause occurs when the stator is saturated. Therefore, there is a subtle difference between the FEM analysis result and the magnetic equivalent circuit analysis result. The displacement stiffness is shown in Figure 3b. At this time, the analysis was performed in the same way as the current stiffness analysis. Displacement stiffness is

an analysis of the magnetic force according to the position in the rotor. The rotor cannot always be positioned exactly in the center. This is because when a magnetic bearing is applied, it floats in the air due to the magnetic force. At this time, if the balance changes slightly, the rotor position will change. The magnetic force acting at this time was analyzed as displacement stiffness. Looking at Figure 3b, it can be seen that the results of the FEM and magnetic equivalent circuit analyses are almost identical. When the rotor position is changed, there is a condition in which the control current applies the same current. Since the important variable for displacement stiffness is the position of the rotor, it was confirmed that there is no significant difference between the fem result and the magnetic equivalent circuit analysis result.

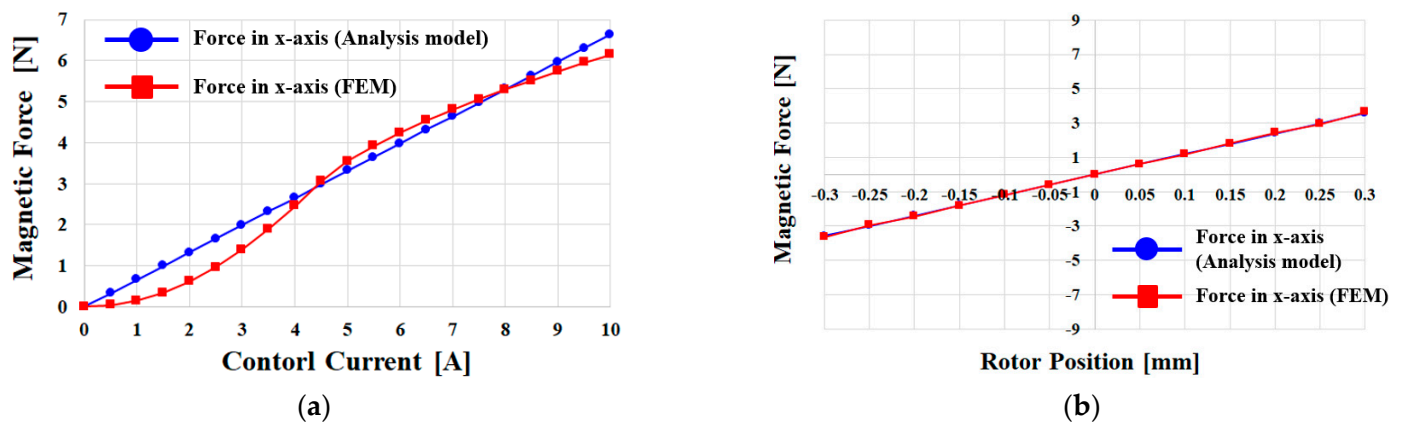


Figure 3. Current stiffness and displacement stiffness for the FEM and magnetic equivalent circuit in the existing model: (a) the force on the x -axis according to the control current and (b) the force on the x -axis according to the rotor position.

3. Performance Analysis of the STMB

Figure 4 shows the shape and major parameters of the STMB. As shown in Figure 4, the STMB consists of four stators in the form of a module. As shown in Figure 4, it can be seen that the STMB has a module structure of four. At this point, key variables arise. Figure 5 shows the main variables and the force according to the variables.

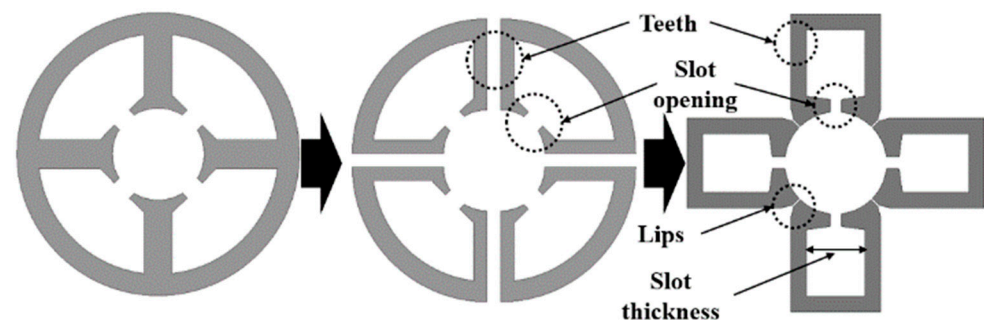


Figure 4. STBM creation process.

The lips part is created by separated stator teeth in the STMB. These lips act as a major variable in the STMB. In addition, the slot opening length also acts as an important variable. Figure 5b shows the force according to the two variable lengths. Both variables showed the same trend. As the length increased, the force decreased. When the lip air gap length increases, the force decreases because magnetic leakage flux occurs between the lips, and even when the slot opening length increases, the magnetic leakage flux occurs between the shoes and the magnetic force decreases. The slot opening length was selected as the minimum while securing the length for the winding wire to enter. The lips air gap length

was selected to be 0.2 mm, and the slot opening length was selected to be 2 mm. At this time, the magnetic force according to the control current in the existing model and the STMB model is shown in Figure 6.

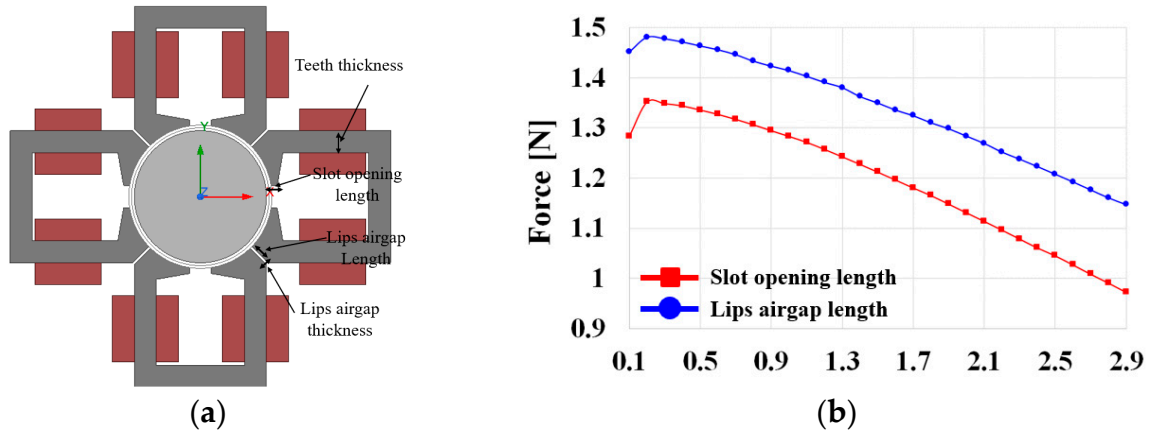


Figure 5. STMB main variable and force according to length: (a) STMB main variable and (b) force according to main variable length.

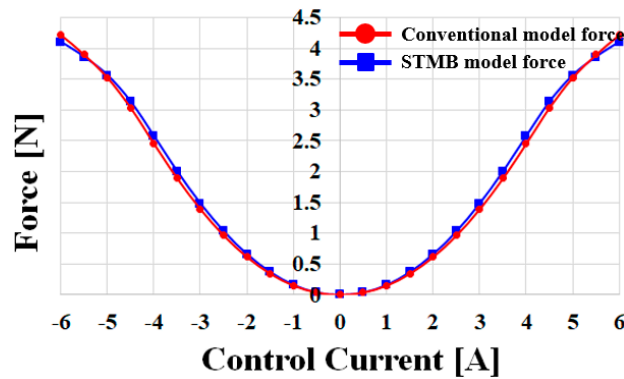


Figure 6. Magnetic force according to the control current of the existing model and the STMB.

Figure 6 shows the magnetic force for the control current of the existing model and the STMB model. The magnetic force for the control current of the conventional model and the STMB has a similar tendency. However, the STMB significantly reduced the stator weight by removing the back yoke by splitting the teeth on the existing stator. The stator weight of the previous model was 54.22 g, but the stator weight of the STMB was 36.15 g, a 33% reduction. Therefore, it is easy to reduce the weight by minimizing iron on the back yoke, and the fill factor is high because there is no restriction on winding. However, since a large leakage magnetic flux occurs between the shoes of the module, the force is reduced. The conventional magnetic bearing and the magnetic flux line of the STMB are shown in Figure 7. Leakage magnetic flux in conventional magnetic bearings occurs at the slot openings, teeth, and back yoke. However, the leakage magnetic flux of conventional magnetic bearings is small and can be ignored. However, the STMB generates a large leakage magnetic flux from slot openings and lips. This is the leakage magnetic flux that occurs between modules. Therefore, in order to reduce the leakage magnetic flux, it is essential to design the main variables. In order to compare the leakage magnetic flux generated from the STMB module, the STMB full model and one STMB module were compared. Both models are shown in Figure 8 and the force for the lip thickness is shown in Figure 9.

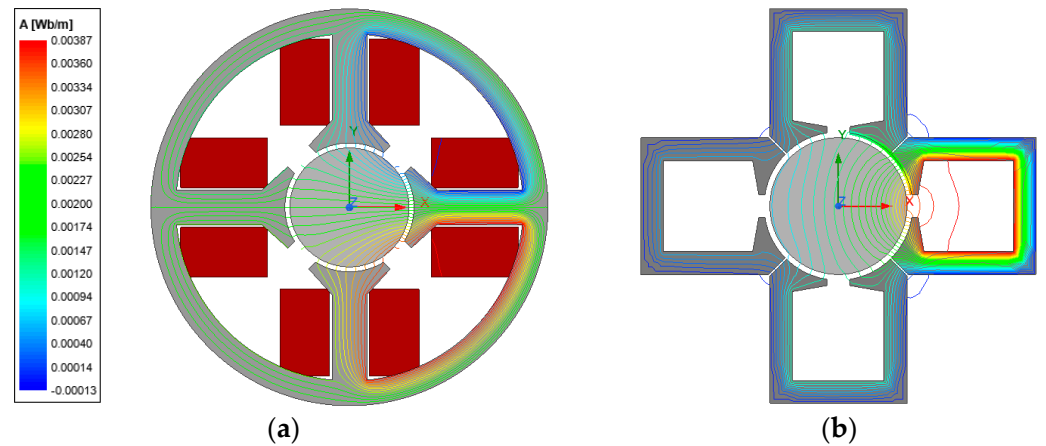


Figure 7. Conventional magnetic bearings and STBM magnetic flux line: (a) conventional magnetic flux line and (b) STMB magnetic flux line.

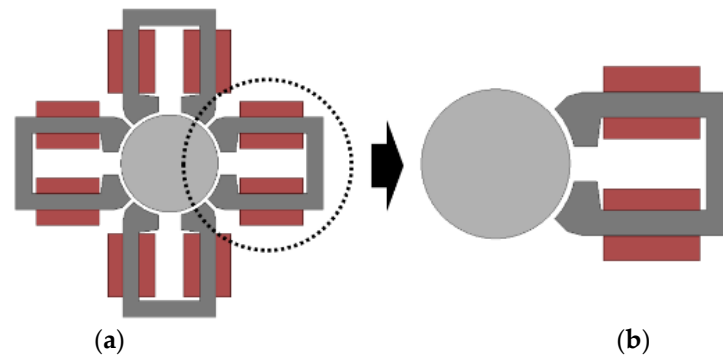


Figure 8. Full module and one-module models: (a) STMB full model and (b) STMB with one module model.

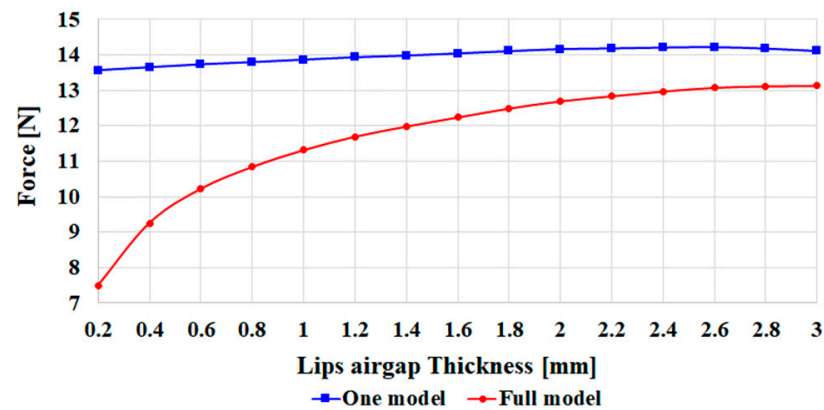


Figure 9. *x*-axis force graph for lip thickness of the full model and the one-module model.

In Figure 9, the single module model has no leakage magnetic flux, so the force is constant even if the lip thickness increases. However, leakage magnetic flux occurs in the ribs between modules in the full module model. Therefore, as the lips thickness increases, the leakage magnetic flux decreases and the force increases. However, it is impossible to prevent leakage magnetic flux from occurring.

4. Hybrid STMB

In the STMB, performance degradation occurs due to leakage magnetic flux generated from the lips. To improve this, this study proposes the HSTMB (hybrid separated teeth

magnetic bearing). The HSTMB is shown in Figure 10 as a model in which a magnet is inserted into the shoe part.

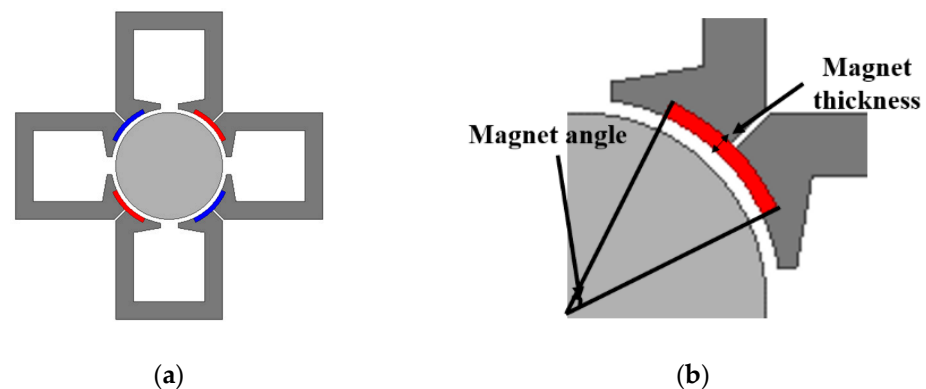


Figure 10. HSTMB full model and variables of the magnet: (a) HSTMB full model and (b) variables of the magnet.

Figure 10 shows the variables of the inserted magnet. Figure 11 shows a graph analyzing the performance depending on the thickness and angle of the magnet. As shown in Figure 11, as the magnet angle increases, the area used for the magnet increases, so the force also increases. However, the magnet thickness is different. The force increases as the magnet thickness increases, but eventually decreases when the magnet thickness increases beyond a certain size. The reason is that the inserted magnet acts as a bias magnet. Therefore, when the thickness of the magnet increases, the magnetic flux generated by the winding acts like an air gap on the inserted magnet with low magnetic permeability, resulting in poor performance. In other words, if the inserted magnet increases, the path of the magnetic flux generated by the winding is obstructed and the force decreases. Therefore, in this study, the magnet angle was selected to be 23 deg and the magnet thickness was selected to be 0.5 mm.

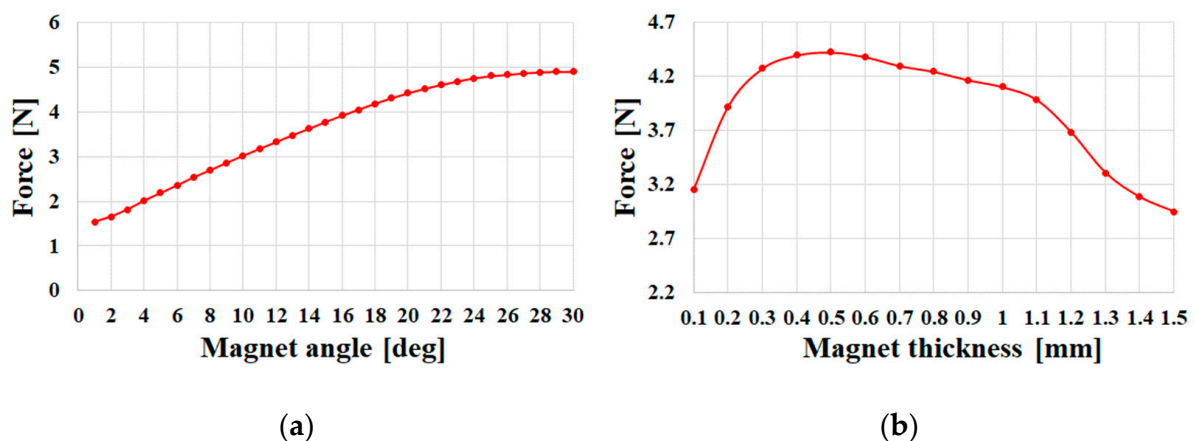


Figure 11. Force analysis depending on variables of the magnet: (a) magnet angle and (b) magnet thickness.

Figure 12 shows the magnetic flux lines of the STMB and HSTMB. The symbol in the figure means the direction of the current. In the case of the STMB, a large leakage magnetic flux occurs between the lips. On the other hand, in the HSTMB, the leakage magnetic flux generated between the lips was significantly reduced by inserting a bias magnet into the shoe. That is, the leakage magnetic flux generated from the lips was reduced due to the inserted bias magnet. Table 2 shows the specifications of the HSTMB. As a specification for the HSTMB, the size was selected to be the same as the existing model. In the HSTMB, the

stator diameter was 40 mm, the rotor diameter was 12 mm, and the air gap was selected to be 0.5 mm. At this time, the number of turns was selected as 40 turns per tooth. The reason is that the HSTMB can secure a high fill factor because it has a stator made by dividing teeth. In this case, heat may be generated in the coil with a high fill factor. However, the HSTMB has an exposed coil structure, which is very advantageous for heat dissipation. The current density is 10.6 A/mm² based on 3A. The variables for the magnet inserted in the shoe part of the stator are the magnet angle and the magnet thickness; the magnet angle is 23 deg and the magnet thickness is 0.5 mm.

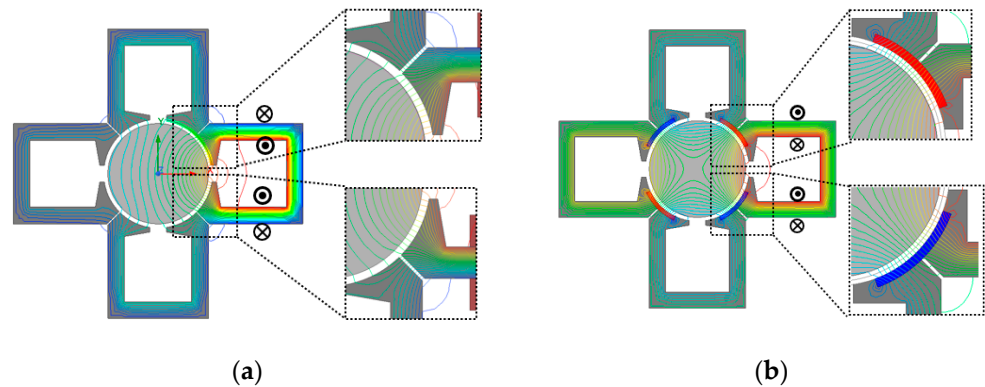


Figure 12. STMB and HSTMB’s magnetic flux line: (a) STMB magnetic flux line and (b) HSTMB magnetic flux line.

Table 2. HSTMB specification.

Parameter	Value	Unit
Stator diameter	40	mm
Rotor diameter	12	mm
Air gap	0.5	mm
Turn	40	-
3A of current density	10.6	A/mm ²
Magnet angle	23	deg
Magnet thickness	0.5	mm

5. Magnetic Equivalent Circuit of the HSTMB

The magnetic equivalent circuit in the HSTMB can be classified into two types. It can be classified into the control magnetic flux generated by winding and Bias Magnetic Flux generated by bias magnetic flux. Figure 13 illustrates the magnetic equivalent circuit of the bias magnetic flux.

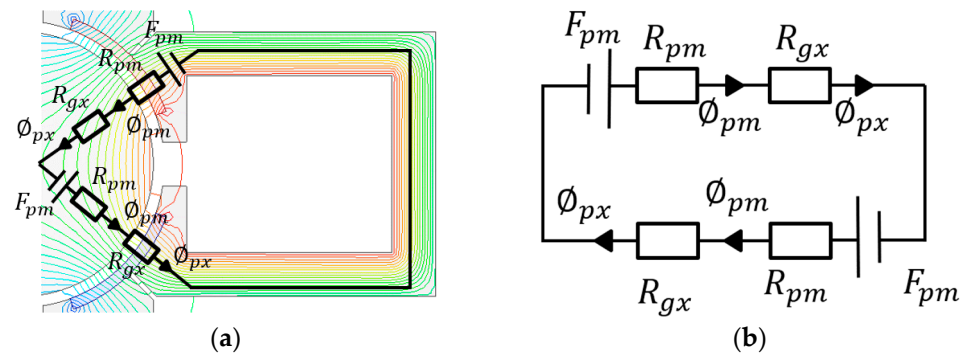


Figure 13. Magnetic equivalent circuit of bias magnetic flux of the HSTMB: (a) magnetic equivalent circuit and (b) the simplified magnetic equivalent circuit.

In Figure 13 F_{pm} , R_{pm} , R_{gx} , ϕ_{pm} , ϕ_{px} mean the magnetomotive force of the magnet, the magneto-resistance of the magnet, the x -axis air gap reluctance, the magnetic flux in the magnet, and the magnetic flux in the air gap, respectively. The formula for the magnetomotive force of a magnet is defined below:

$$F_{pm} = H_{pm}h_{pm} \tag{5}$$

H_{pm} and h_{pm} mean the coercive force and the length of the magnet, respectively. The formula for magneto-resistance is defined below:

$$R_{pm} = \frac{F_{pm}}{\mu_0\mu_r A_{pm}}, R_{gx} = \frac{g+x}{\mu_0}, \tag{6}$$

$$R_{sum} = R_{pm} + R_{gx}$$

A_{pm} is the area of the magnet and R_{sum} is the total magnetic resistance. x is the radial displacements as the rotor deviates away from its center position along the x -axis. μ_r is the relative permeability, μ_0 is the permeability in vacuum, and g is the air gap length. Figure 14 illustrates the magnetic equivalent circuit for the control magnetic flux.

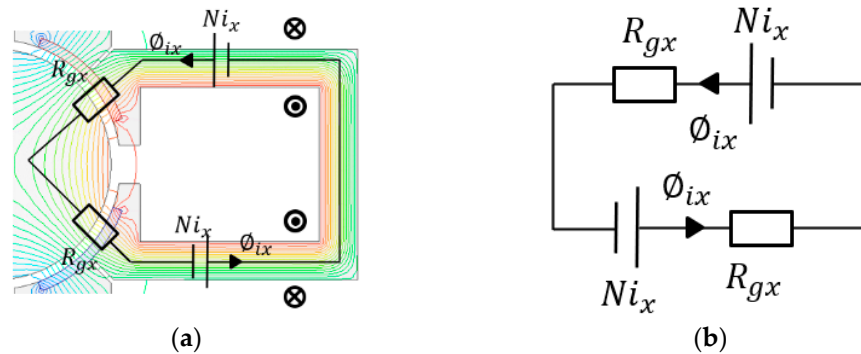


Figure 14. Magnetic equivalent circuit of the control magnetic flux of the HSTMB: (a) magnetic equivalent circuit and (b) the simplified magnetic equivalent circuit.

In the magnetic equivalent circuit shown in Figure 14, ϕ_{ix} means the control magnetic flux. The formula is defined below:

$$\phi_{ix} = \frac{Ni_x}{R_{gx}} \tag{7}$$

The magnetic force acting on the HSTMB can be obtained using the formula obtained above. The magnetic force of the HSTMB is defined in Equation (8):

$$f_x = \frac{1}{2\mu_0 A_r} ((\phi_{ix} + \phi_{px})^2) \tag{8}$$

A simple and effective way to analyze the dynamic characteristics of the HSTMB and to control its stability is to linearize the nonlinear magnetic force about the nominal operating point using a first-order Taylor series for small values of f_x . The formula of applying the first Taylor series to i_x and x is as follows:

$$f_x \cong \left. \frac{\partial f_x}{\partial i_x} \right|_{i_x = i_y = 0, x = y = 0} \cdot i_x + \left. \frac{\partial f_x}{\partial x} \right|_{i_x = i_y = 0, x = y = 0} \cdot x \tag{9}$$

where k_{ri} and k_r are the force–current stiffness and the force–displacement stiffness of the RMB unit on the x -axis, respectively, and they can be derived and given by the formula below:

$$\begin{cases} k_{ri} = \frac{\mu_0 H_c h_m N_r}{2g \left(\frac{h_m}{A_m \mu_r} + \frac{g}{A} + \frac{g}{A_{pm}} \right)} \\ k_r = \frac{\mu_0 (H_c h_m)^2}{4Ag^2 \left(\frac{h_m}{A_m \mu_r} + \frac{g}{A} + \frac{g}{A_{pm}} \right)} \end{cases} \quad (10)$$

In Figure 15, the force on the x -axis of the force–current stiffness and the force–displacement stiffness are compared with the results of the analysis model and the FEM simulation results.

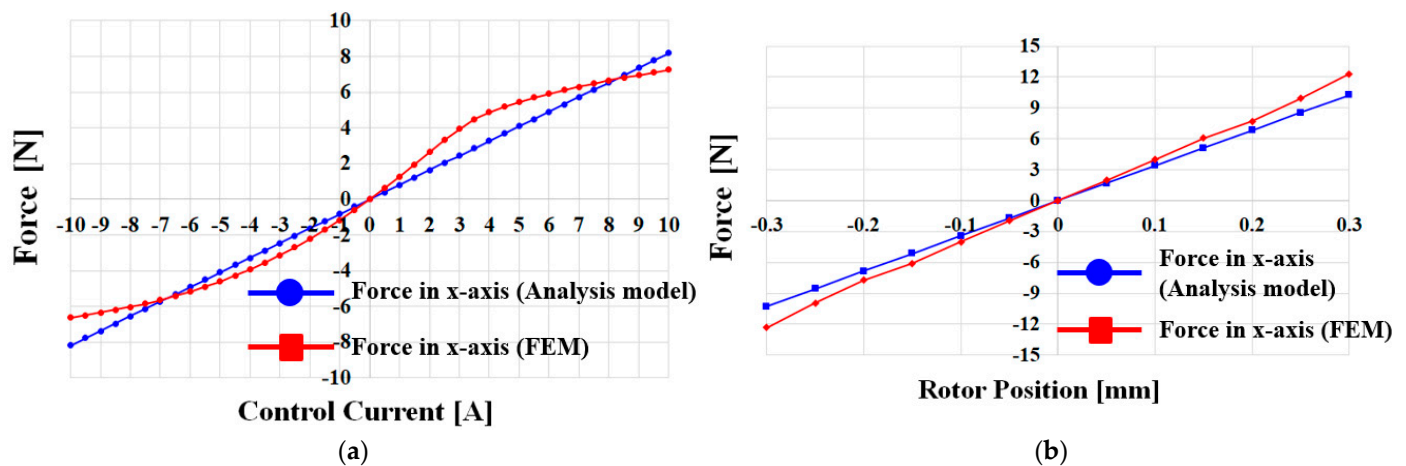


Figure 15. Force–current stiffness and the force in the HSTMB: (a) the force on the x -axis according to the control current and (b) the force on the x -axis according to the rotor position.

Figure 15a shows the force depending on the current. The analysis model results through the magnetic equivalent circuit and the FEA simulation results were compared. It can be seen that the tendency of current stiffness for the two analysis methods are similar. Therefore, it can be regarded as a valid result. The FEA simulation results are the result values including saturation of the core and leakage magnetic flux. (b) shows the force depending on the rotor position. A comparison was made using the same two methods as in (a). The tendency of displacement stiffness for the two methods is similar, and it can be confirmed that it is a valid result value. The FEA simulation results are the result values including saturation of the core and leakage magnetic flux. Compared to Figure 3b, the force is different according to the rotor position. Figure 3b shows no difference, Figure 15b shows a difference. The reason is that Figure 3b is a very simple structure with a general magnetic bearing. Only force by the control current exists. Therefore, there is no significant difference between the FEA and magnetic equivalent circuit analyses. However, in Figure 15b, there is a difference between the FEA and magnetic equivalent circuit analyses because the force caused by the control current and the bias magnet inserted into the stator occurs. In addition, a larger difference occurs because the leakage magnetic flux is not considered in the bias magnet.

Figure 16 shows the force according to the current in the conventional model and the HSTMB model. In Figure 16, the current–force of the HSTMB model has a larger overall effect than that of the conventional model. Table 3 shows the comparison of performance and weight with the conventional model and the HSTMB. In the same size standard, the force increased by about 2.1 times from 1.3 [N] to 4.1 [N] at 3A of current density. In addition, the total weight decreased by about 15.1% from 109.78 [g] to 95.35 [g]. That is, the magnetic force increased and the weight decreased under the same size. A large copper loss occurs as a large current is applied to the coil of the magnetic bearing. Accordingly, a

lot of heat is generated in the coil. Many problems occur due to the heat generated from the coil. Therefore, the heat dissipation structure also plays an important role. Since the HSTMB structure is a structure in which the stator is separated, the coil is exposed outside the stator. This is because the back yoke is removed by separating the teeth of the stator. Since the coil is exposed in the remaining space after removing the back yoke and winding is performed by dividing the coil into several teeth, it is very advantageous for the heat dissipation structure. A heat dissipation structure can be added to the exposed coil. In addition, since it was originally an empty space, the size does not increase. Compared to the previous model, the HSTMB has a very advantageous heat dissipation structure. At this time, the turns shown in Table 3 are turns per teeth. Since the HSTMB is a model with twice as many teeth as the conventional model, the HSTMB is larger than the conventional model in terms of the number of equivalent serial turns. Therefore, it can be confirmed that the dong weight goes out more. However, the HSTMB has thinner teeth and is wound in two places, so there is no significant difference in weight or loss. In addition, it can be confirmed that the core weight decreases more rapidly than the copper weight increases, reducing by about 15% in terms of the total weight. In addition, heat generation problems may occur due to the use of a lot of copper, but HSTMB has an advantageous structure for heat dissipation because it has a structure in which the coil is exposed.

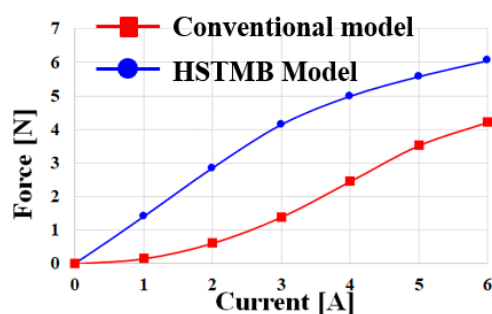


Figure 16. Force–current stiffness and the force in the HSTMB.

Table 3. Comparison of Conventional model and HSTMB model specifications.

Parameter	Conventional Model	HSTMB Model	Unit
Stator diameter	40	40	mm
Rotor diameter	12	12	mm
Air gap	0.5	0.5	mm
Turn	35	40	-
3A of current density	10.6	10.6	A/mm ²
3A of force	1.3	4.1	N
Copper weight	55.56	59.2	g
Core weight	54.22	36.15	g
Total weight	109.78	95.35	g

6. Conclusions

Recently, digitalization is progressing in various industries. For this reason, many technical studies on high-speed, light-weight, high-output, and high-efficiency motors are being conducted. Here, in the case of high-speed motors, research on bearings as well as motors is being conducted. When a motor rotates at high speed, various disadvantages such as large loss and shortened life occur due to the friction generated in the bearing. As a bearing to compensate for this, there is a magnetic bearing. Because the magnetic bearing uses magnetic force, it can compensate for the disadvantages of the existing bearings. However, it has disadvantages such as being heavy and expensive. In this study, the STMB (separated teeth magnetic bearing) was proposed by dividing the teeth part of the existing magnetic bearing in order to reduce the weight of the magnetic bearing. However, STMB

generates a large leakage magnetic flux in the lip part, causing performance degradation. Because the STMB is made by dividing the stator teeth, a back yoke does not exist. This is because the lips play the role of the back yoke at this time. However, the magnetic flux generated by the control current in the lips part causes leakage through the lips and reduces the magnetic force. This study proposes the HSTMB to supplement the disadvantages of the STMB. The HSTMB (hybrid separated teeth magnetic bearing), a structure with a bias magnet inserted in the shoe part, improves performance by reducing the leakage magnetic flux generated in the lips part. At this time, the magnet thickness and magnet angle of the bias magnet inserted into the shoe act as major variables. As the magnet thickness increases, the bias magnetic flux increases, but the magnetic flux generated by the control current decreases. Because the magnetic flux by the control current feels like a gap in the bias magnet, it appears as a phenomenon that obstructs the magnetic flux path. Therefore, analysis is essential as appropriate thickness is required. In addition, since the effective area of the magnetic angle increases, performance improves as it increases. However, manufacturability must be considered. If it is designed too large, the thickness of the shoe becomes thin, which can cause problems with rigidity. Thus, in this paper, the force–current stiffness and the force–displacement stiffness were analyzed using a magnetic equivalent circuit and FEA, and valid results were proven. Finally, based on 3A, the magnetic force increased by about 3.2 times from 1.3 [N] to 4.1 [N] compared to the conventional model, and the weight was reduced by about 15.1% from 109.78 [g] to 95.35 [g].

Author Contributions: Conceptualization, S.-W.S.; Methodology, S.-W.S.; Software, S.-W.S.; Formal analysis, S.-W.S.; Investigation, S.-W.S.; Writing—original draft, S.-W.S.; Writing—review & editing, S.-W.S.; Visualization, W.-H.K. and D.-H.J.; Supervision, W.-H.K., J.L. and D.-H.J.; Project administration, S.-W.S. and W.-H.K. All authors have read and agreed to the published version of the manuscript.

Funding: This work was supported by a National Research Foundation of Korea (NRF) grant funded by the Korean government (MSIT). (No. 2020R1A2C1013724), and in part by Korea Electric Power Corporation. (Grant number: R22XO02-02).

Data Availability Statement: Not applicable.

Conflicts of Interest: The authors declare no conflict of interest.

References

1. Wang, X.; Zhang, Y.; Gao, P. Design and Analysis of Second-Order Sliding Mode Controller for Active Magnetic Bearing. *Energies* **2020**, *13*, 5965. [[CrossRef](#)]
2. Rao, P.N.; Devarapalli, R.; García Márquez, F.P.; Malik, H. Global Sliding-Mode Suspension Control of Bearingless Switched Reluctance Motor under Eccentric Faults to Increase Reliability of Motor. *Energies* **2020**, *13*, 5485. [[CrossRef](#)]
3. Liu, G.; Liu, X. Integrated Design of a High Speed Magnetic Levitated Brushless Direct Current Motor System. *Energies* **2018**, *11*, 1236. [[CrossRef](#)]
4. Siamaki, M.; Storey, J.G.; Wiesehofer, L.; Badcock, R.A. Design, Build, and Evaluation of an AC Loss Measurement Rig for High-Speed Superconducting Bearings. *Energies* **2022**, *15*, 1427. [[CrossRef](#)]
5. Duan, R.; Liao, Y.; Yang, L.; Song, E. Faulty Bearing Signal Analysis With Empirical Morphological Undecimated Wavelet. *IEEE Trans. Instrum. Meas.* **2022**, *71*, 3508711. [[CrossRef](#)]
6. Trinh, M.H.; Van Tran, Q.; Ahn, H.-S. Minimal and Redundant Bearing Rigidity: Conditions and Applications. *IEEE Trans. Autom. Control.* **2020**, *65*, 4186–4200. [[CrossRef](#)]
7. Wang, H.; Liu, K.; Wei, J.; Hu, H. Analytical Modeling of Air Gap Magnetic Fields and Bearing Force of a Novel Hybrid Magnetic Thrust Bearing. *IEEE Trans. Magn.* **2021**, *57*, 4900107. [[CrossRef](#)]
8. Zhao, S.; Zelazo, D. Bearing Rigidity and Almost Global Bearing-Only Formation Stabilization. *IEEE Trans. Autom. Control.* **2016**, *61*, 1255–1268. [[CrossRef](#)]
9. Xu, J.; Chen, R.; Hong, H.; Yuan, X.; Zhang, C. Static Characteristics of High-Temperature Superconductor and Hydrodynamic Fluid-Film Compound Bearing for Rocket Engine. *IEEE Trans. Appl. Supercond.* **2015**, *25*, 3601908. [[CrossRef](#)]
10. Yamagishi, K. Optimum Design of Integrated Magnetic Bearing Using Multiple HTS Bulk Units. *IEEE Trans. Appl. Supercond.* **2019**, *29*, 6801505. [[CrossRef](#)]
11. Zhang, T.; Bao, P. Design of the Six-Pole Hybrid Magnetic Bearing with Separated Magnetic Circuit to Generate Symmetrical Levitation Force. *IEEE Trans. Appl. Supercond.* **2021**, *31*, 5205804. [[CrossRef](#)]

12. Jiang, H.; Su, Z.; Wang, D. Analytical Calculation of Active Magnetic Bearing Based on Distributed Magnetic Circuit Method. *IEEE Trans. Energy Convers.* **2021**, *36*, 1841–1851. [[CrossRef](#)]
13. Zhang, T.; Wang, Z. Structure and Levitation Force Characteristics Analysis for Novel Radial Hybrid Magnetic Bearing. *IEEE Trans. Appl. Supercond.* **2021**, *31*, 0602705. [[CrossRef](#)]
14. Han, B.; Zheng, S.; Li, H.; Liu, Q. Weight-Reduction Design Based on Integrated Radial-Axial Magnetic Bearing of a Large-Scale MSCMG for Space Station Application. *IEEE Trans. Ind. Electron.* **2017**, *64*, 2205–2214. [[CrossRef](#)]
15. Ju, J.; Xu, P.; Li, S.; Xu, T.; Ju, F.; Du, J. Design and Optimization Method with Independent Radial and Axial Capacity for 3-DOF Magnetic Bearings in Flywheel. *Energies* **2023**, *16*, 483. [[CrossRef](#)]
16. Zhang, W.; Wang, Z. Accurate Modeling and Control System Design for a Spherical Radial AC HMB for a Flywheel Battery System. *Energies* **2023**, *16*, 1973. [[CrossRef](#)]
17. Haidl, P.; Buchroithner, A. Design of a Low-Loss, Low-Cost Rolling Element Bearing System for a 5 kWh/100 kW Flywheel Energy Storage System. *Energies* **2021**, *14*, 7195. [[CrossRef](#)]
18. Le, Y.; Sun, J.; Han, B. Modeling and Design of 3-DOF Magnetic Bearing for High-Speed Motor Including Eddy-Current Effects and Leakage Effects. *IEEE Trans. Ind. Electron.* **2016**, *63*, 3656–3665. [[CrossRef](#)]
19. Fang, J.; Xu, S. Effects of Eddy Current in Electrical Connection Surface of Laminated Cores on High-Speed PM Motor Supported by Active Magnetic Bearings. *IEEE Trans. Magn.* **2015**, *51*, 8207604. [[CrossRef](#)]
20. Prasad, K.N.V.; Narayanan, G. Electromagnetic Bearings With Power Electronic Control for High-Speed Rotating Machines: Review, Analysis, and Design Example. *IEEE Trans. Ind. Appl.* **2021**, *57*, 4946–4957. [[CrossRef](#)]
21. Le, Y.; Wang, K. Design and Optimization Method of Magnetic Bearing for High-Speed Motor Considering Eddy Current Effects. *IEEE ASME Trans. Mechatron.* **2016**, *21*, 2061–2072. [[CrossRef](#)]
22. Schuck, M.; Nussbaumer, T.; Kolar, J.W. Characterization of Electromagnetic Rotor Material Properties and Their Impact on an Ultra-High Speed Spinning Ball Motor. *IEEE Trans. Magn.* **2016**, *52*, 8204404. [[CrossRef](#)]
23. Looser, A.; Kolar, J.W. An Active Magnetic Damper Concept for Stabilization of Gas Bearings in High-Speed Permanent-Magnet Machines. *IEEE Trans. Ind. Electron.* **2014**, *61*, 3089–3098. [[CrossRef](#)]
24. Song, S.-W.; Yang, I.-J.; Lee, S.-H.; Kim, D.-H.; Kim, K.S.; Kim, W.-H. A Study on New High-Speed Motor That Has Stator Decreased in Weight and Coreloss. *IEEE Trans. Magn.* **2021**, *57*, 8201105. [[CrossRef](#)]
25. Song, S.-W.; Pyo, H.-J.; Lee, J.; Kim, W.-H. A study on Radial Magnetic Bearing of a new stator shape for high manufacturability and reduction of weight. In Proceedings of the 2022 IEEE 20th Biennial Conference on Electromagnetic Field Computation (CEFC), Denver, CO, USA, 24–26 October 2022; pp. 1–2. [[CrossRef](#)]

Disclaimer/Publisher’s Note: The statements, opinions and data contained in all publications are solely those of the individual author(s) and contributor(s) and not of MDPI and/or the editor(s). MDPI and/or the editor(s) disclaim responsibility for any injury to people or property resulting from any ideas, methods, instructions or products referred to in the content.